ELSEVIER

Journal of Power Sources 52 (1994) 99–108

JOURNAL OF POWER SOURCES

Cycle life test of lead dioxide electrodes in compressed lead/acid cells

Johan Landfors

Department of Chemical Engineering, Division of Applied Electrochemistry, The Royal Institute of Technology, 100 44 Stockholm, Sweden

Received 3 May 1994; accepted 27 May 1994

Abstract

Flat pasted lead dioxide electrodes of SLI-type have been studied in compressed lead/acid batteries and tested with respect to cycle life and polarization during galvanostatic charge and discharge cycling. Three different sets of separators have been tested in order to verify the importance of the applied mechanical pressure and the effects of using separators with different permeability. It was found that it was possible to increase the life from about 90 cycles for a non-pressurized cell with standard separators to about 1150 cycles for a pressurized cell with a multilayer separator with a thin polyester fabric closest to the lead dioxide electrode. Cells with glass-fiber mats closest to the lead dioxide electrodes had a lifetime of about 750 cycles. It was found that the changes in the cell voltages with increasing cycle number could be correlated to transformation of the active material and loss of lead dioxide due to shedding. Further, it was observed that the reasons for cell failure were closely related to the permeability of the separators and the applied pressure. It is also concluded that flat pasted electrodes in pressurized cells could be a very attractive alternative to cells with tubular lead dioxide electrodes.

Keywords. Lead/acid battery, Lead dioxide; Porous electrodes; Cycle life; Pressurized cells

1. Introduction

Although all lead/acid batteries are based on the same overall reaction, the construction of optimized batteries depends to a large extent on their specific application. The requirements of stationary compared with traction batteries are quite different. Batteries suitable for electrical vehicles need high energy density combined with high cycle life and mechanical strength, while power back-up systems primarily have to be robust and reliable. Desired properties, e.g., high power density and high cycle life, are often difficult to combine in the same cell. Therefore, the development of batteries is often a matter of finding the most suitable compromise for a particular application. However, independently of where the battery is operating, the lifetime is always an important issue in order to make it economically favourable compared with other sources of electrical energy.

Another feature common to most lead/acid batteries is that the performance to a large extent is governed by the positive plates. The lead dioxide electrodes are generally more sensitive to acid depletion at high discharge current densities than are the negative plates. Also with respect to the cycle life, lead/acid batteries are often limited by the life of the lead dioxide electrodes.

The most common reasons for cell failure due to the positive plate are shedding or sludging, grid corrosion and passivation by formation of lead sulfate that cannot be oxidized back to lead dioxide [1–7]. In order to increase the cycle life of the PbO_2 electrodes, it is therefore important to minimize the effects of these three factors by finding suitable grid alloys, cell designs and properties of the active material. This paper deals primarily with how the cycle life can be increased by changing the cell design in order to prevent shedding and sludging.

It has been reported in several papers that the cycle life can be dramatically increased if the active material is immobilized by physically pressing it against the current collector with an externally applied force. This prevents shedding and maintains the electrical contact between lead dioxide particles even after deep-discharge cycles. The pressure also improves the electrical contact between the current grid and the active lead dioxide

SSDI 0378-7753(94)01944-O

if corrosion products or lead sulfate are formed in the interface between them.

Retaining the lead dioxide is an old idea used in tubular plate electrodes where the active material is enclosed in a cylindrical electrolyte permeable fabric [8–11]. Batteries with tubular positive plates are very robust and have a service life of up to 2000 to 3000 cycles. The power and energy densities are however not comparable to, e.g., SLI batteries. The production cost is also rather high compared with the pasted alternatives.

Compression of the active material can also be obtained in batteries with plane electrodes by exerting an external pressure perpendicular to the electrode plates [1,12–14]. This can be achieved in batteries with separators of glass fibers, e.g., sealed batteries [15–22] or some other material with pores small enough, to prevent lead dioxide particles from falling off the plate [1,12,13]. Up to 3000 charge and discharge cycles were accomplished in cells with pasted plane electrodes and a multilayer separator consisting of a microporous separator against the positive plate, a glass-fiber mat closest to the negative plate and in the middle a corrugated and perforated polyvinyl chloride (PVC) separator [12,13].

Therefore, the aim of this investigation was to verify the experimental results obtained in pressurized lead/acid cells and confirm if the cycle life can be greatly increased for ordinary SLI electrode plates. Further, we wanted to compare different types of separators, their effect on the cycle life and the reasons for cell failure, e.g., shedding, grid corrosion and passivation. Studies of changes in electrochemical behaviour and composition of the active material were used to correlate the performance with structural changes and passivation of the electrodes.

2. Experimental

The electrodes used in this study were commercially available SLI electrodes manufactured by TUDOR AB in Nol, Sweden. The grids were alloyed with 2.5% Sb and the electrode dimensions were 115 mm × 155 mm (height × width). The thickness of the electrodes were 1.8 and 2.2 mm for the negative and the positive electrodes, respectively. Some trials were also performed with lead electrodes with a thickness of 4 mm in order to make sure that the positive electrode was the limiting one, both with respect to the discharge capacity and the cycle life. The electrodes were cut out from full size electrode plates to a dimension of 115 mm × 40 mm (height × width). All electrodes were cut from the same part of the full size plates so that they had an identical shape and the plate lug could be used for welding on lead wires with a diameter of 3 mm.

The cell packages were assembled from three negative and two positive plates electrically connected in parallel to form four electrode gaps. The lead electrode placed in the middle consisted of two plates in order to ensure overcapacity for the negative electrodes. A set of different separators were used in each cell. The following separator setups were used:

A. A single polyethylene separator for starter batteries, Daramic 350 manufactured by GRACE. These cells were operated as reference trials without any external pressure.

B. A combination of three separators with a microporous cellulose separator closest to the negative electrode, a glass-fiber mat (BG 200 17 Hollingsworth and Vose) against the positive and between them a coarse monofilament polyester fabric (Polymon PES 840/46, mesh size 840) in order to evenly distribute the applied mechanical pressure.

C. The same as in B but with the glass-fiber mat changed to a dense monofilament polyester fabric (Polymon PES 125/35, mesh size 125). The aim of the setup was to make a parallel to how tubular electrodes are designed, i.e., with a fabric preventing the lead dioxide from falling off the plate and at the same time give better access to the free electrolyte than in cells with glass-fiber mats. A schematic of the separator setup is presented in Fig. 1.

Two cells of configuration A and B, respectively, and three cells of C were tested with respect to the cycle life. Notations A1, B1 and C1 refer to cells with standard lead electrodes while the cells A2, B2 and C3 all had thick lead electrodes.

The electrode packages were mounted into flexible polyethylene bottles with a volume of 1 l and held plane parallel with the sides of the bottle by blocks of polymethylmetacrylate (PMMA). The mechanical pressure was applied by a screw clamp with a calibrated spring. The applied pressure could thus be monitored by measuring the compression of the spring. The applied

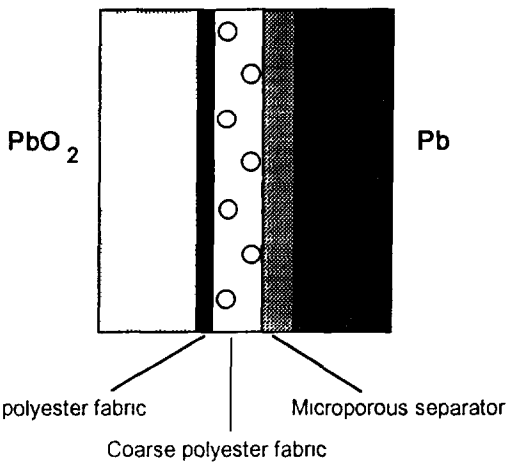

Fig. 1 The separator setup used in the pressurized cells of type C.

pressure was 10^5 Pa for all cells of the configurations B and C. This has been reported as a suitable pressure for compressed cells with flat electrodes [1,12,13]. A schematic of the complete cell assembly is shown in Fig. 2.

The cells were filled with 5.0 M sulfuric acid (Merck, AR) up to about 1 cm over the top of the electrode packages. The electrolyte concentration was kept constant (±2%) by addition of water from a combined Milli-RO 15 and Milli-Q water purification system from millipore. The top of the cell container was covered with a polymer film to avoid evaporation and acid spray gases. In order to maintain a uniform concentration in the free electrolyte, air was blown through a polyethylene tube introduced from the top down to the bottom of the container. The electrolyte was mixed in this way for 30 min every two hours.

The cells, kept at room temperature 22±1 °C, were automatically cycled in a galvanostatic mode. The cell voltages were continuously monitored on *x–t* recorders during cycling according to the following scheme:

1. Initial charge with a current density of 54.2 A m^{-2} to oxygen evolution
2. Resting period 3600 s
3. Discharge with 144 A m^{-2} for 5500 s, corresponding to about 75% depth-of-discharge (DOD) of cell type C, or until the cell voltage reached 1.7 V
4. Resting period 100 s
5. Recharge with 54.2 A m^{-2} for 18 000 s, corresponding to 23% overcharge
6. Back to 2 if the discharge time $t_d > 4400$ s. Thus, the cycling was stopped when the discharge capacity was reduced to 60% of the initial capacity of cell type C.

The discharge capacities reported below have been normalized by dividing by the discharge capacity used during cycling, i.e., 220 Ah m^{-2}.

After the cycling, the sulfuric acid was poured out and the cells were carefully disassembled. The electrodes were leached in acetone or purified water in order to remove the sulfuric acid. After leaching, the electrodes were dried at 50 °C. The separators were leached in water and dried at ambient temperature.

The distribution of lead sulfate across the thickness of the electrodes was studied with an electron-probe microanalyzer (ARL SEMQ 42) by recording the intensity of the S Kα radiation. Samples of the electrodes were moulded in to an epoxy resin, polished with diamond paste and sputtered with carbon before the analyses. Analyses were performed on fully charged electrodes to determine the amount of sulfur that could not be recharged. The average sulfur concentrations in the electrodes were calculated from the measured sulfur profiles.

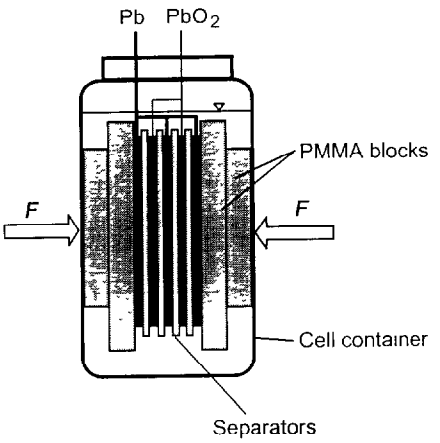

Fig 2 Complete cell system with electrolyte container.

3. Results and discussion

3.1. Initial discharge capacities

The discharge capacity as a function of the current density was thoroughly determined only for cell configuration C. The results are presented in Fig. 3 which shows the average DOD of the lead dioxide as a function of the discharge current density to a cell voltage of 1.7 V. As can be expected, the discharge capacity decreases with increasing current density. Fig. 3 is based on a limited number of observations and shows a qualitative rather than quantitative relationship. However, the average discharge capacity at 144 A m^{-2} is based on three different measurements and could be determined to 365±20 A s g^{-1} PbO_2, corresponding to a discharge time of about 2.02 h. All cells were cycled at 75% of this discharge capacity in order to have a comparable utilization of the active mass in all three cell configurations.

Fig. 4 show how the cell voltages of the three different cell configurations varied with time during the 20th galvanostatic discharge. it can be seen that cell type A has the best discharge characteristics, followed by cell B and then cell C. In order to compare the cells, the energy output, *W*, was calculated by integration of the discharge curves according to the equation:

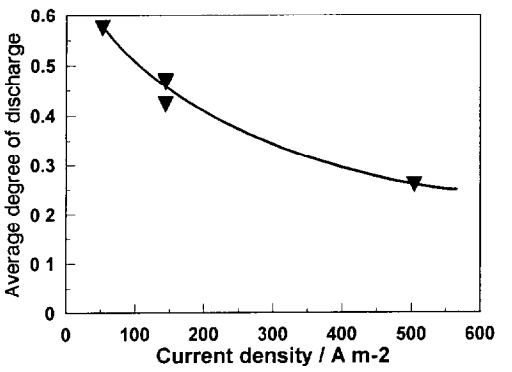

Fig. 3. Discharge capacity vs. current density for cell type C.

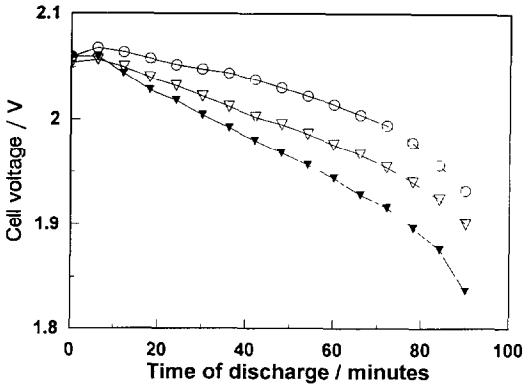

Fig. 4. Cell voltage vs. time during galvanostatic discharge at 144 A m^{-2} for (○) cell A, (△ cell B and (▼) cell C. The data were collected during cycle number 20 for cells with thin lead electrodes.

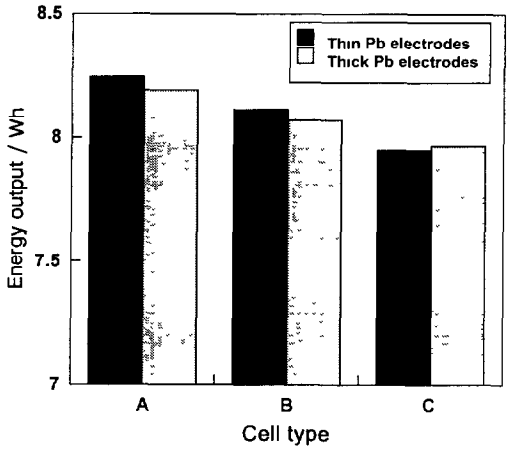

Fig. 5 Energy output from the cells during the 20th discharge cycle.

$$W = \int_{t=0}^{t_d} IU(t)\,dt \quad (1)$$

where I is the cell current, U the cell voltage, and t the time of discharge until end of discharge, t_d.

The results are presented in Fig. 5. It can be seen that the energy output from the pressurized cells, B and C, is slightly lower compared with the standard cell A. The decrease compared with configuration A is about 1.5 and 3.1% for the cells B and C, respectively. The differences can be explained mainly by the increased ohmic resistance caused by the additional separators. It can further be seen that the differences between cells with thin and thick lead electrodes are small, less than 0.7%. Also, there is no clear correlation between the type of lead electrode used and the energy output in the different cells. Although the number of observations are strongly limited, it can be concluded that the choice of lead electrode does not seem to have any large impact on the energy output.

It must be noted that the results in Figs. 4 and 5 do not reflect the maximum discharge capacity since the cells were never completely discharged. A comparison with respect to discharge capacity would have told much more about the effect of the separators on the transport of acid from the free electrolyte into the porous electrodes although high transport resistance in a cell is always reflected by a higher ohmic drop and lower cell voltage. However, deep discharges at different current densities would have affected the electrodes and made it difficult to draw any extensive conclusions from the cycle life tests. This is also further discussed in connection with the cycle life tests.

Also, a more detailed discussion in order to explain the voltage characteristics and the discharge capacities for different cells, would require a complete mathematical model to describe the current distribution and transport phenomena in the electrodes as well as the separators. However, that is beyond the scope of this paper.

3.2. Cycle life test

The results from the galvanostatic long-term experiments are summarized in Figs. 6 to 8. Fig. 6 shows how the normalized discharge capacity changed during cycling of cells A1 and A2. It can be seen that the capacities were maintained up to about 60 cycles before they started to decrease. The fact that both cells behaved in the same way, indicates that the capacity is limited by the lead dioxide electrodes and not by the lead electrodes since the negative electrodes in cell A2 were heavily oversized. If the failure was due to the negative electrodes, there would probably have been a large difference in cycle life. When the cell was disassembled, large amounts of lead dioxide were found on the bottom of the cell container. No visual changes could be identified on the negative electrodes, except for a slight increase in thickness. Thus, it can be concluded that the cycle life of non-pressurized cells with standard separators is limited by shedding under the specified cycling conditions. A maximum life of about 90 charge and discharge cycles is also what can be expected for

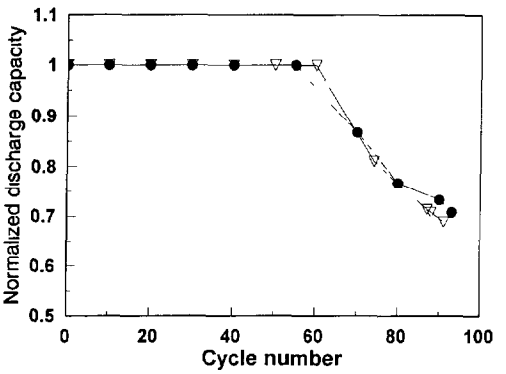

Fig. 6. Normalized discharge capacities vs. cycle number for (●) cells A1 and (▽) A2.

commercially available SLI batteries and for sealed lead/acid batteries [15].

The cycle life can probably be increased considerably by applying a more sophisticated recharge procedure including a potentiostatic period at the end of the charge. The galvanostatic recharge procedure used in these trials probably caused a lot of unnecessary shedding due to fairly long periods of oxygen evolution at 54.2 A m^{-2}.

For cell configuration B the behaviour is rather different compared with the standard cells, see Fig. 7. The discharge capacities were maintained during the first 700 cycles for both cells before they almost simultaneously started to decrease very drastically to reach about 750 cycles before the discharge capacity had decreased below 80%. Also in these cases, any limitation due to the negative electrodes can be excluded on the same reasons as for cell configuration A. No sludge was found in the electrolyte when the cell was disassembled. It is therefore concluded that all shedding was prevented by the glass-fibre mats pressed against the positive plates. When separating the electrodes, it was found that all grids in the positive electrodes in both cell B1 and B2 had been cut off by severe corrosion about 2 cm from the top of the electrodes. Therefore, it could be concluded that the reason for cell failure was grid corrosion of the positive electrodes.

It is difficult to offer a complete explanation for the highly reproducible corrosion effects. It could be possible that the compressed glass-fiber mats closest to the positive electrodes decreases the accessibility of sulfuric acid. Thus, the acid depletion causes accelerated dissolution of lead from the grid during anodic polarization. Another possible explanation could be that oxygen is trapped in the upper parts of the positive electrodes and the compressed glass-fiber mats during charge These parts could thus be electrically isolated, causing a non-uniform current distribution over the exterior surface of the lead dioxide electrodes and a more pronounced corrosion in the zone just below the gas pocket.

Nevertheless, it can be concluded that the cycle life can be greatly improved by compressing the cell with a microporous separator closest to the positive electrode in order to prevent shedding. The use of glass-fiber mats can however cause accelerated local corrosion of the current grid. Maybe it could be possible to reduce the negative effects of the mat by reducing the pressure. That could lead to a more open structure of the glass fibers and at the same time improve the transport of acid and gas in the system. It is also possible that a different cycling procedure could improve the corrosion situation. A deeper understanding of these phenomena could be a suitable objective for further research in this area.

In order to facilitate a good accessibility of sulfuric acid to the electrodes and at the same time avoid shedding by compression, the glass-fiber mat was changed to a thin monofilament polyester fabric, cell configuration C. The results from the galvanostatic long-term trials are presented in Fig. 8. It can be seen that cell configuration C managed to withstand about 1150 cycles before reaching the limit of 80% residual capacity. Cell C2 had a very stable performance before the capacity dropped quickly, while the capacity of cell C1 varied between 82 and 135% capacity. The drop in capacity of cell C1 after about 250 cycles is probably due to some of the discharge capacity tests that were performed down to a cell voltage of 1.7 V at the beginning of the trial. However, the cell managed to withstand 1150 cycles before the trial was ended due to short circuiting caused by lead dendrites from the lead electrode. From examination of cell C2 it was concluded that the reason for cell failure was grid corrosion. However, the corrosion attack was not as localized as for the cell configuration B.

The effect of deep discharges on the long-term stability can also be seen for cell C3 that was exposed to a large number of complete discharges (cutoff voltage of 1.7 V). The discharge capacity decreased quickly with increasing cycle number. After about 500 cycles, the capacity stabilized at about 40 to 50% capacity. Despite the low capacity, the trial was continued and terminated

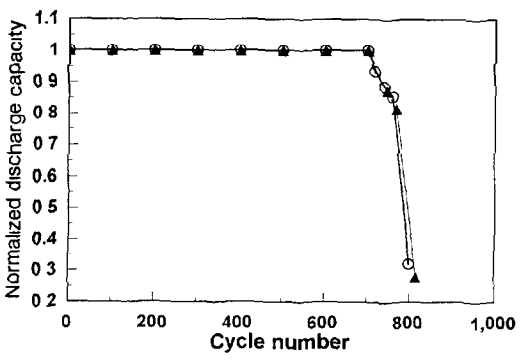

Fig. 7. Normalized discharge capacities vs cycle number for (○) cells B1 and (▲) B2.

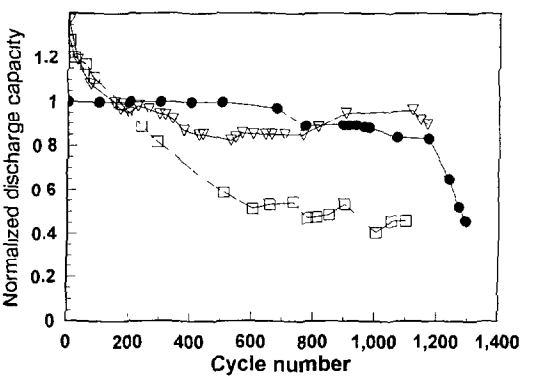

Fig 8 Normalized discharge capacities vs. cycle number for (▽) cells C1, (●) C2 and (□) C3

after 1097 cycles due to short circuiting caused by dendrites from the lead electrode.

From cell C1 and C3, both subjected to deep-discharge cycles, it seems obvious that high polarization of the electrodes, which was the case during deep-discharge cycles, could be detrimental to the long-term stability of the cells. Repetitive cycling can reduce the electrical contact between lead dioxide particles due to large changes in the morphology [1,23,24]. Deep cycles also have a negative impact on the corrosion layer between the current grid and the active mass that could cause irreversible changes [2,3]. The results also illustrate the importance of exposing the cells to identical cycling schemes to obtain comparable data on cycle life performance during cycling.

Some limited shedding was observed for all cells of configuration C. Some of the lead dioxide sludge had been trapped in the coarse polyester fabric and some on the bottom of the cell container. However, most of the lead dioxide was still in contact with the lead dioxide electrodes.

The results from the long-term trials are summarized in Fig. 9. It can be clearly seen that the cycle life of the positive electrode can be substantially increased by applying an external pressure and at the same time facilitate a fairly good accessibility of sulfuric acid from the separator region into the lead dioxide electrode. A too large diffusion resistance, as was the case for the cells with glass-fiber mats, seems to result in an accelerated corrosion rate of the current grid. This is also in agreement with what was reported in Ref. [23] where it was stated that positive plates wrapped with glass-fiber mats normally fail due to grid corrosion rather than to loss or degradation of the active material. Therefore, it seem obvious that further improvements can be made by optimization of the space closest to the positive electrode by finding the best combination between permeability for acid and tendency for shedding.

The fact that the cycle life is dramatically increased by applying an external pressure is well in accordance with the results by Alzieu et al. [12,13] and Tsubota [22]. Alzieu et al. used a microporous separator welded around the positive plate and achieved cycle lives of about 3000 cycles at 10^5 Pa. At the same time they used a charge cycle with galvanostatic charge followed by a constant voltage of 2.70 V for 90 min which probably gave less oxygen evolution compared with this work.

The cell used by Alzieu et al. [12,13] seems to be similar to the cell types B or C used in this investigation, although we did not achieve more than about 750 and 1150 cycles, respectively. Even though there probably are some differences in cell design, it could be possible that the extensive overcharge used in this investigation was unsuitable for a cell with a dense separator against the lead dioxide electrode. If that is the case, it can be assumed that a cell with a more open separator against the positive plate, e.g., cell type C, can withstand gas evolution better and maybe be recharged much faster than a cell with a microporous separator closest to the lead dioxide electrode.

3.3. Discharge curves

A more detailed analysis of changes in the lead dioxide electrodes can be performed by studying individual discharge curves for the cell configurations during different stages of the cycle life. Fig. 10 shows how the cell voltage varied with time for the standard cell A1 during different cycles. It can be clearly seen how the polarization at the later stage of the discharge increases with increasing cycle number. After 50 cycles, the polarization at the end of the discharge is about 100 mV higher compared with the curve for the 20th cycle. After about 60 cycles, the discharge capacity decreases drastically. However, the initial polarization, during approximately the first 20 min, did not change very much during the trial. In fact, a small decrease in the polarization could be noted during the first 50

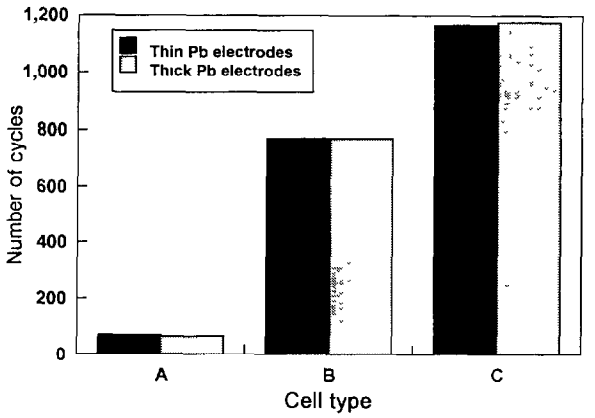

Fig 9. Number of cycles obtained for the different cell configurations.

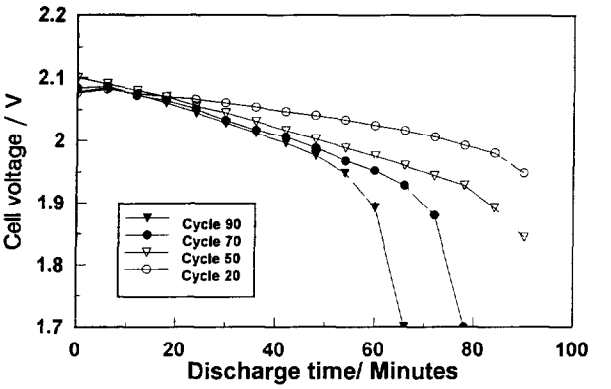

Fig 10 Cell voltage vs time during discharge of cell A1 during different cycles

cycles. At the end of the life, the cell voltage increases and the capacity is strongly reduced. It can be seen that the capacity seems to be limited by the amount of available reactants, most probably lead dioxide. This was also verified by the large amount of lead dioxide found on the bottom of the cell, as discussed above.

The discharge curves for cell B1 show a somewhat different picture, see Fig. 11. It can be seen that the polarization characteristics were maintained during the first 500 cycles and then decreased drastically when the effects of the grid corrosion became significant. Thus, it can be concluded that most of the lead and the lead dioxide in cell configuration B was electrochemically active during most of the cycling period. The shapes of the discharge curves were fairly similar indicating that the loss of active material or changes in the mass transport were fairly small. Instead of increasing polarization with increasing cycle number, as was the case for cell configuration A, the polarization during the first 30 min of the discharge actually decreased with increasing cycle number, except for cycle number 500.

From the discharge curves for cell configuration C, see Fig. 12, it can be seen that the behaviour is similar to the non-pressurized cells, with a decreasing discharge capacity with increasing cycle number, except for the fact that the decrease in capacity could be postponed by more than ten times. In the same way as for cell configuration B, the initial polarization decreases during the first 200 cycles before it starts to increase, while the polarization at the end of discharge increases with increasing cycle number. This indicates a slow but continuous passivation or loss of active material.

The changes in the discharge curves at the end of the discharge fit well with observed shedding for the different cell types. The non-pressurized cells had severe shedding and consequently the polarization increased drastically with cycle number at the end of the discharge. The cell with the tightest separator against the lead dioxide electrode, cell type B, had almost no shedding and consequently the polarization at the end of the discharges were almost unchanged except for the very last cycles when the grid corrosion was severe. Cell type C seems to be an intermediate case compared with the configurations A and B. It has a high cycle life, some limited shedding and the polarization at the end of the discharge cycle increases slightly with increasing cycle number.

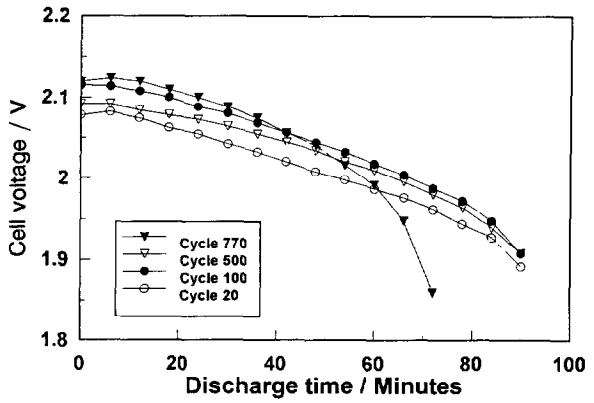

Fig. 11. Cell voltage vs. time during discharge of cell B1 during different cycles.

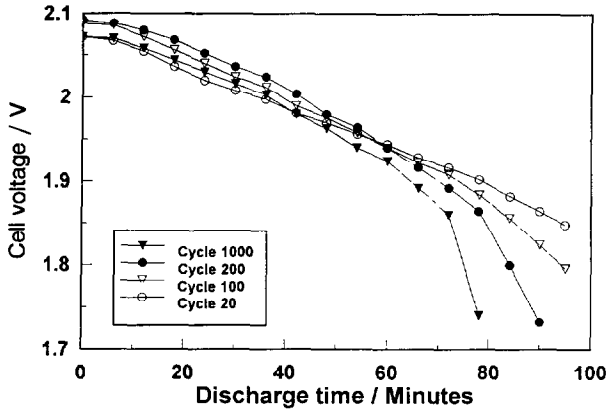

Fig. 12. Cell voltage vs. time during discharge of cell C1 during different cycles

3.4. Initial cell voltages

The fact that the polarization during the first 20 min seems to decrease during the first 50 to 100 cycles for all cells, indicate that there is some general improvement of the cell performance due to the repetitive cycling. In order to study this in greater detail, the cell voltages after 6 min of discharge have been plotted versus the cycle number, see Figs. 13 to 15. From Fig. 13 it can be seen that the cell voltages improve during cycling of the cell type A. The upper curve, for the cell with thin lead electrodes, has a maximum at about 50 cycles before the voltage starts to decrease slightly. The lower curve, for the cell with thick lead electrodes, shows a similar behaviour but without any distinct maximum.

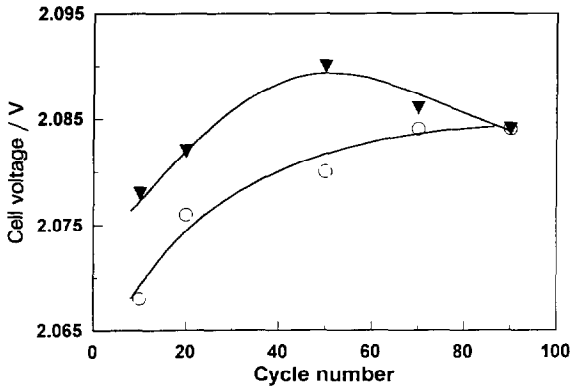

Fig. 13. Changes in cell voltage at 6 min of discharge during cycling of cell type A with (▼) thin lead electrodes and thick (○) lead electrodes

In both cases, the improvement in cell voltage is in the range of 10 to 15 mV.

The improved voltage with increasing cycle number is probably an effect of a more favorable morphology of the porous active materials, the lead and/or the lead dioxide. Another effect giving a decreased polarization could be that the volume of the lead electrode increases during cycling, thus decreasing the electrode distance and the ohmic drop. With a current density of 144 A m^{-2} and assuming a conductivity of 79 Ω^{-1} m^{-1} and a maximum swelling of 0.5 mm on each side of the electrode, the improvement in cell voltage would only correspond to about 1 mV. An improvement in the order of 100 to 150 mV must therefore be explained mainly by the changes of the properties of the active mass and not by a decreased electrode gap.

The initial cell voltages versus cycle number for cell type B are shown in Fig. 14. The cell with thin lead electrodes shows a similar behavior as the cell with thick lead electrodes although the voltage is about 15 to 20 mV lower for the latter. The first 100 cycles are similar to cell type A with an improvement of the cell voltage of about 10 mV. The cell voltage is then rather stable during the major part of the cycling except for the last period when there is some further improvement of cell voltage. It must, however, be emphasized that the last period was operated with strongly corroded grids and with reduced discharge capacity.

Also cell configuration C showed an improvement of the cell voltage during the initial period of cycling, see Fig. 15. However, compared with both cell types A and B the decrease in polarization is larger, about 30 and 15 mV for the cell with thin and thick lead electrodes, respectively. After reaching a maximum, the cell voltages were fairly stable before they started to decrease slightly with increasing cycle number. The decrease in cell voltage during the later stage can probably be explained by the successive loss of active material or phase transformation to permanent sulfate crystals or inactive lead dioxide forms.

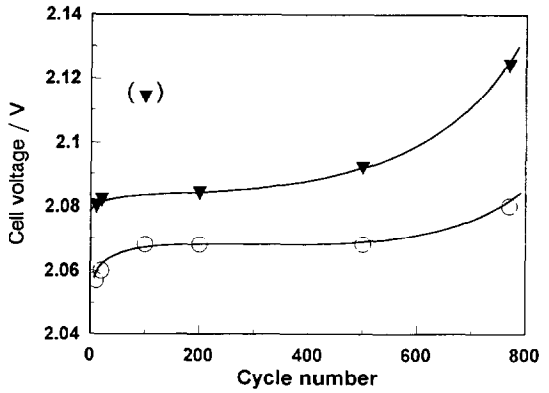

Fig. 14. Changes in cell voltage at 6 min of discharge during cycling of cell type B with (▼) thin lead electrodes and (○) thick lead electrodes.

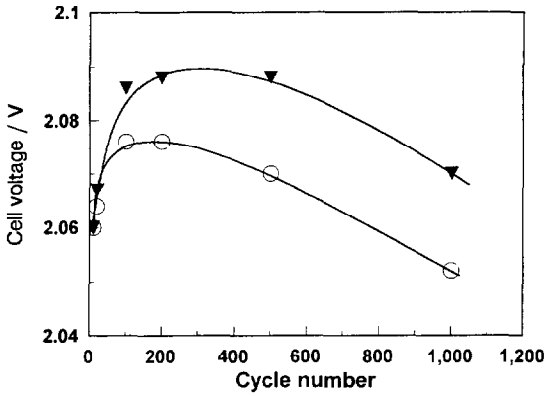

Fig. 15. Changes in cell voltage at 6 min of discharge during cycling of cell type C with (▼) thin lead electrodes and (○) thick lead electrodes

The data shown in Figs. 13 to 15 indicate that the cycling period can be divided into two different stages:

(i) an initial period during the first 100 cycles when the properties of the porous electrodes are improved to give a lower polarization, and

(ii) a second stage when the polarization increases with increasing cycle number due to either loss of active material or formation of inactive lead sulfate or oxides; the reasons for the decrease in performance probably depend on the cell configuration and the applied pressure.

Changes of the properties of the active mass during cycling of lead/acid batteries have previously been discussed in the literature [1,12,13]. In Refs. [12] and [13] it was observed that the average pore radius in a lead dioxide electrode increased from about 0.15 to about 0.4 μm during the first 500 to 700 cycles for a pressurized lead/acid cell. Continued cycling showed that the average pore radius was fairly constant or slightly decreasing up to about 3000 cycles. The shape of the curve, showing average pore radius as a function of cycle number published in Ref. [13], is very similar to the evolution of the initial cell voltage that was found for cell type C in the present investigation. Thus, it seems reasonable to assume that the changes in initial cell voltage during cycling is closely related to changes of the morphology of the active material.

In Ref. [1] Takahashi et al. found that cycling of pressurized cells led to increased porosity and decreased active surface area. However, during their trials the positive active material was allowed to expand from about 3.4 to about 4 mm which makes it difficult to make a comparison with the present work. Takahashi et al. [1] also found that the cycling resulted in an increase in the volume fraction of large pores. An increase that could be suppressed by increasing the mechanical pressure of the cell. This is in accordance with the results obtained in Refs. [12] and [13] and suggests that the improvement in cell voltage during

cycling could be explained by a more favorable pore-size distribution, which also would affect the active surface area of the active material.

From what has been reported [1,12,13,22] is it obvious that the magnitude of the applied mechanical pressure is crucial for the cycle life. Alzieu et al. [12,13] reported an optimal pressure of 10^5 Pa for their set of separators. In the present investigation, the main focus has been given to the effects of separators on the cycle life at a constant pressure. However, from what has been found, it seems reasonable to believe that each specific set of separators has its own preferred working pressure to obtain highest cycle life.

The behavior of lead dioxide electrodes during cycling depends on a large number of factors. It has been demonstrated that pressure and separator design are important parameters. The transformation of lead dioxide has a very large effect on the cell voltage and on the contact between lead dioxide particles. It is clear that further development of cycle life analyses of lead dioxide electrodes would require more sophisticated models for how the morphology changes and how this affects the electrode kinetics during cycling.

Further development of high cycle life lead/acid cells also requires the application of mathematic models for prediction of discharge capacities and recharge characteristics. Such models would have to take into consideration the effects of separator regions with different permeability in order to model cells with extremely high cycle life.

3 5. *Electron-probe microanalysis*

Fig. 16 shows the average sulfur concentrations in the lead dioxide electrodes in the different cell types. It can be seen that the sulfur content is lowest for cell type A and highest for cell type C. If it is assumed that the sulfur content is related to the amount of lead sulfate that cannot be oxidized, the results indicate that the degree of deactivation increases with increasing cycle number. Even though the limited number of cells studied makes it difficult to draw any quantitative conclusions, it seems like the passivation is a continuous process that is caused mainly by the cycling and to a lesser extent by the cell configuration or the applied pressure.

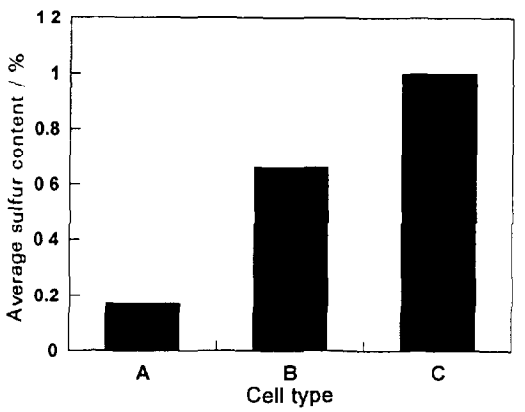

Fig 16 Average sulfur concentrations in charged lead dioxide electrodes after completed cycling

The increase in lead sulfate content in the positive plates with increasing cycle number is also in agreement with other investigations. Chang [24] explained the build-up of inactive sulfate as an important factor for cell failure. Harris et al. [25] reported an almost linear increase of the lead sulfate content in charged positive plates with increasing cycle number.

4. Conclusions

From the results and discussions above, it can be concluded that the cycle life of lead dioxide electrodes subjected to extensive overcharge can be greatly improved by applying an external pressure perpendicular to the electrode plates. The cycle life depends to a large extent on the properties of the separators and on the applied pressure. Separators with high transport resistance should be avoided to reduce grid corrosion.

Suitable separators have a combination of layers with different properties to optimize the cycle life of both the negative and positive electrode. A thin microporous separator is preferred closest to the lead electrode to avoid lead dendrites due to repetitive cycling. The separator closest to the lead dioxide electrode should have a fairly dense structure to prevent shedding. At the same time the separator must be fairly thin and open to facilitate good mass transfer of electrolyte as well as gases during charge and discharge. Suitably, a third coarse region is added between the separators closest to the electrodes to act as an electrolyte reservoir and to evenly distribute the applied pressure over the electrode surface. It is also important to allow for gas release if the rate of gas formation is higher than the recombination rate at the opposite electrode.

The changes of the active materials during cycling can be divided into three different main processes that influence the performance of the electrodes during different stages of the life:

(i) improvement of the morphology of the active materials which leads to higher cell voltage and higher energy output;

(ii) loss of active material due to shedding or decreased contact between particles of the active material which lead to increased polarization and lower discharge capacity, and

(iii) deactivation by formation of large lead sulfate crystals that cannot be recharged under normal charge procedures.

It is important to get a suitable balance between (i) and (ii) in order to achieve high cycle life. It has been shown that multilayer separators can be used to meet these requirements.

The application of composite separators and pressurized cells is an attractive alternative to other batteries with high cycle life, e.g., cells with tubular lead dioxide electrodes. The use of pasted electrodes offers a simplified production and potentially lower production costs compared with other alternatives.

Acknowledgements

This work was financially supported by the Swedish National Board for Technical Development. Dr R. Aronsson, TUDOR AB, is greatfully acknowledged for supplying the electrodes and the microporous separators used in this study.

References

[1] K Takahashi, M. Tsubota, K. Yonezu and K. Ando, *J. Electrochem Soc*, *130* (1983) 2144.
[2] B.K. Mahato, *J Electrochem Soc*, *126* (1979) 365.
[3] G. Papazov, T. Rogatchev and D Pavlov, *J Power Sources, 6* (1981) 15.
[4] D. Barret, M.T. Frost, J.A. Hamilton, K. Harris, I.R. Harrowfield, J.F. Moresby and D.A.J. Rand, *J. Electroanal Chem*, *118* (1981) 135.
[5] Z. Takehara, K. Kanamura and M Kawanami, *J Electrochem Soc., 136* (1989) 620.
[6] D. Berndt, in J. O'M. Bockris (ed.), *Comprehensive Treatise of Electrochemistry,* Vol. 3, Plenum, New York, 1981.
[7] H. Bode, *Lead–Acid Batteries,* Wiley-Interscience, New York, 4th edn., 1977.
[8] A. Lindholm, *J. Power Sources, 10* (1983) 71.
[9] A. Lindholm, *J. Appl Electrochem*, *13* (1983) 693.
[10] J. Landfors and D. Simonsson, *J. Electrochem. Soc*, *139* (1992) 2760.
[11] J. Landfors and D. Simonsson, *J. Electrochem Soc., 139* (1992) 2768.
[12] J. Alzieu, N. Koechlin and J. Robert, *J Electrochem Soc*, *134* (1987) 1881.
[13] J Alzieu and J. Robert, *J Power Sources, 13* (1984) 93.
[14] M. Tsubota, S. Osumi and M. Kosai, *J. Power Sources, 33* (1991) 105.
[15] C.H. Harman and J Lim, *J. Power Sources, 33* (1991) 25.
[16] Y. Fujita, *J Power Sources, 19* (1987) 175
[17] B. Culpin and J.A. Hayman, *15th Int. Power Sources Symp*, *1986.*
[18] K Mori and K Asai, *GS News, 44* (1985) 5.
[19] K. Mori and K Asai, *GS News, 44* (1985) 11
[20] M. Maja and N. Penazzi, *J Power Sources, 25* (1989) 229
[21] H. Dietz, M. Radwan, J. Garche, H. Doring and K Wiesener, *J. Appl. Electrochem., 21* (1991) 221.
[22] M. Tsubota, *New Mater. New Process., 2* (1983) 107.
[23] N.J. Maskalick, *J Electrochem Soc*, *122* (1975) 19.
[24] T G. Chang, *J. Electrochem. Soc*, *131* (1984) 1755
[25] K. Harris, R.J. Hill and D.A.J. Rand, *J Power Sources, 8* (1982) 175